

Retinal disease identification using upgraded CLAHE filter and transfer convolution neural network

Sinan S. Mohammed Sheet^{a,*}, Tian-Swee Tan^b, M.A. As'ari^b, Wan Hazabbah Wan Hitam^c,
Joyce S.Y. Sia^b

^a Technical Engineering College of Mosul, Northern Technical University, Mosul, Iraq

^b School of biomedical engineering and health sciences, University Technology Malaysia, Johor, Malaysia

^c School of Medical Sciences, Health Campus, University Sains Malaysia, Kelantan, Malaysia

Received 23 December 2020; received in revised form 24 March 2021; accepted 2 May 2021

Available online 8 May 2021

Abstract

Retinal tissue plays a crucial part in human vision. Infections of retinal tissue and delayed treatment or untreated infection could lead to loss of vision. Additionally, the diagnosis is prone to errors when huge dataset is involved. Therefore, a fully automated model of identification of retinal disease is proposed to reduce human interaction while retaining its high accuracy classification results. This paper introduces an enhanced design of a fully automatic multi-class retina diseases prediction system to assist ophthalmologists in making speedy and accurate investigation. Retinal fundus images, which have been used in this study, were downloaded from the stare website (157 images from five classes: BDR, CRVO, CNV, PDR, and Normal). The five files were categorized according to their annotations conducted by the experienced specialists. The categorized images were first processed with the proposed upgraded contrast-limited adaptive histogram filter for image brightness enhancement, noise reduction, and intensity spectrum normalization. The proposed model was designed with transfer learning method and the fine-tuned pre-trained RESNET50. Eventually, the proposed framework was examined with performance evaluation parameters, recorded a classification rate with 100% sensitivity, 100% specificity, and 100% accuracy. The performance of the proposed model showed a magnificent superiority as compared to the state-of-the-art studies.

© 2021 The Korean Institute of Communications and Information Sciences (KICS). Publishing services by Elsevier B.V. This is an open access article under the CC BY-NC-ND license (<http://creativecommons.org/licenses/by-nc-nd/4.0/>).

Keywords: Retinal disease; Retinal fundus images; Convolution neural network (CNN); (CLAHE) filter

1. Introduction

Eye is the main organ in human vision. It bonds several mutual anatomical and physiological links with the brain which is protected by a skeletal rampart. Human eye has fibrous layers and a twin blood resource that connect to the specific nervous layer in the retina. The internal cavities of eye and brain are filled with fluids that are of similar formation and under comparable pressures, where infections could affect both eye and central nervous system. Therefore, physicians should stay aware of illness conditions that incline to simultaneously implicate the patient's eye and the nervous system [1].

Fig. 1 shows five classes of retinal images for healthy eye and of different disease progressions. In fact, leaving retinal illness without receive any treatment may cause blindness in several cases [2]. According to Hagiwara et al. the physicians determine imperfections in the visual part with boundary tracking, typically perimeter measurement to evaluate the width of the cornea, tonometry in incorrect intraocular pressure detection, and ophthalmoscopy device in tracking the glaucomatous optic circle [3]. These testing processes can only be carried out by trained ophthalmologists. Nonetheless, the retinal diseases diagnosis was generally made by analyzing and evaluating the captured retina images, and hence the procedure could be time-consuming, even for skillful ophthalmologists [4]. Meanwhile, the global increment in the number of patients with eye problem might exacerbate the situation in delayed disease detection. Kaur et al. claimed that about a 0.4 million blindness in the world had been detected while 2.6 million patients faced critical vision weakness in 2015 due to retina

* Corresponding author.

E-mail addresses: Sinan_sm76@ntu.edu.iq (S.S.M. Sheet), tantswee@utm.my (T.-S. Tan), sari@biomedical.utm.my (M.A. As'ari), hazabbah@usm.my (W.H.W. Hitam), ssyjoyce2@live.utm.my (J.S.Y. Sia).

Peer review under responsibility of The Korean Institute of Communications and Information Sciences (KICS).

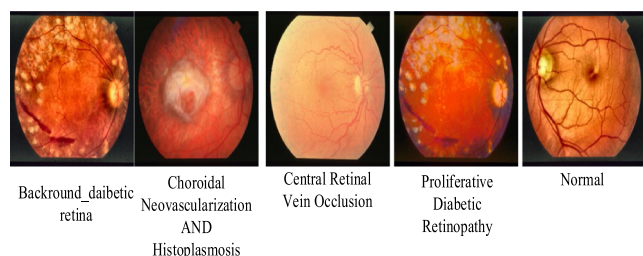


Fig. 1. Sample of the five different image classes: BDR, (CNV&Hist), CRV, PDR, and Normal.

diseases [5]. In short, the tedious diagnosis process could possibly lead to severe retinal tissue impairments and the risk of human error during the investigation procedures.

On the contrary, the computer-aided automatic diagnosis model shows strong capability in solving the aforementioned drawbacks and potentially to be referred as a major approach in recent studies [4]. Transforming from human inspection into machine inspection imposes more novel approaches in processing medical images typically disease analysis with multilane classification. Retinal illnesses include eyes ailments, brain tumor ailments, breast cancer ailments, rectum ailments, and heart ailments [6]. The techniques that are commonly implemented in retina photography are “fluorescein angiography, optical coherence tomography (OCT) and Color stereographic photography”. Additionally, newer technologies have become more widely applied to capture the fundus images due to their simplicity, wide accessibility, and their utility in offering color images which are crucial in documentation [2,7].

Machine inspection (neural network hypothesis) involves a variety of procedures, for instance a classifier in distinguishing multiple illnesses among image datasets [5,8,9], and a trained model in extracting set of features in differentiating the retinal diseases [10–12]. In medical image processing, the specialists have been increasingly focusing on the intervention of AI (Artificial Intelligent) in analysis, disease diagnosis and prediction [13,14]. Additionally, DL (Deep Learning) methods have delivered impressive contributions in yielding accurate results in diagnosis and prediction of pulmonary tuberculosis from chest X-ray images and diabetic retinopathy (DR) [15,16]. Notably, eye illnesses have two leading phases in the recent studies. The first phase aims to detect the symptoms of diabetic retinopathy (DR) (including glaucoma, age-related macular degeneration, retinopathy of prematurity, and refractive error). The second phase is a new research area that deals with a new variety of retinal illnesses, for instance choroidal-neovascular [CNV], macular degeneration AMD, and diabetic macular edema (DME) [12]. The automated diagnosis models are assisted with CNN in disease identification (Convolution Neural Network) [17–20].

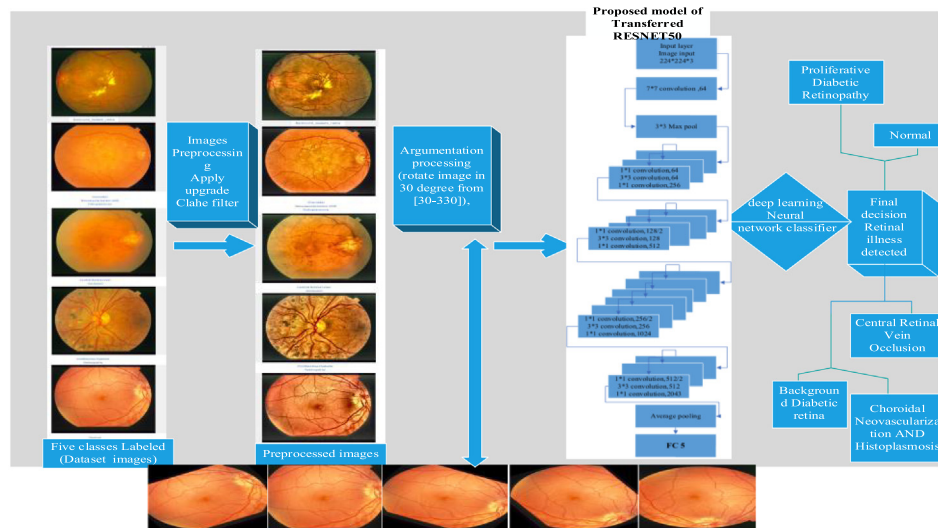
Introduced by [21], Contrast-Limited Adaptive Histogram Equalization (CLAHE) filter was proven to be effective in improving the micro-aneurysms pixels. There are two methods for image contrast enhancement to improve veins' contrast [22]. First, CLAHE filter manages to produce adequate enhancement in veins, and remains robust in dealing with

noisy environments. The filter performs better than other global enhancement approaches, such as conventional contrast extending and general histogram equalization. The second method in improving vein's contrast is by using independent element analysis. Recent studies have included several image enhancement techniques in pre-processing stage that includes the procedure as follows: image grayscale conversion, spectrum normalization, brightness improvement with CLAHE and gamma adjustment to improve the overall appearance. The third pre-processing step target to enhance the (foreground–background) contrast of the entire dataset [23]. The procedure eventually ends with data augmentation. An explicitly designed contrast enhancement method named Prominent Region of Interest (RoI) Contrast Enhancement (PROICE) was proposed to improve the distinctiveness of the RoI's sub-distribution [24]. However, the majority pixels of fundus images were black pixels which might experience excessive enhancement effect that could distort the image overall visibility. Long et al. claimed that the accuracy of MA recognition is closely related to the image quality [25], and hence further pre-processing steps are required. CLAHE is normally applied to improve the distinctiveness between the background and the tinted dark areas (BVs, HMs, and MAs in the shade-corrected image).

Transfer learning based on pre-trained network reveals a remarkable improvement in network accuracy, and it is exclusive to train a network with smaller datasets, especially the case of medical imaging.

Generally, the transfer learning technique is a process to reuse the ready neural networks that have been applied in other applications. Additional refining processes are required to recognize new object areas (such as detection of glaucoma in fundus pictures). To fine tune the networks, the weights of original design are referred as the initial marks, then they are adjusted to translate the pre-trained networks to be more relevant in another object recognition (for instance, the transformed network “Image-Net” that used to detect general images in, detecting retinal images) [12]. D. Le et al. [26] presented a study to assess the viability of deep learning in identifying diabetic retinopathy from the dataset of coherence tomography angiography with the transfer learning method based on pre-trained VGG16 networks for strong OCTA classification. In normal circumstances, common CNN requires substantial amount of training set which is less feasible in training labeled medical images due to its high demand from experts in annotations and limited samples of data. Therefore, X. Li et al. suggested to screen small datasets by using the transfer learning technique in the four pre-trained networks, namely Alex-Net, Vgg-s, VggNet-vd-16, and VggNet-vd-19 [27]. The optimized pre-trained networks focus on extracting the fundus features that are later fed to the support vector machine (SVM) classifier to minimize the overfitting problem that might be invoked in training small dataset. Prokofyeva offered notable contributions in generalizing a series of pre-processing steps for deep transfer learning when the information is inadequate [28].

In this work, a novel design of an automated retinal diseases detection model to identify a variety of eye illnesses has been



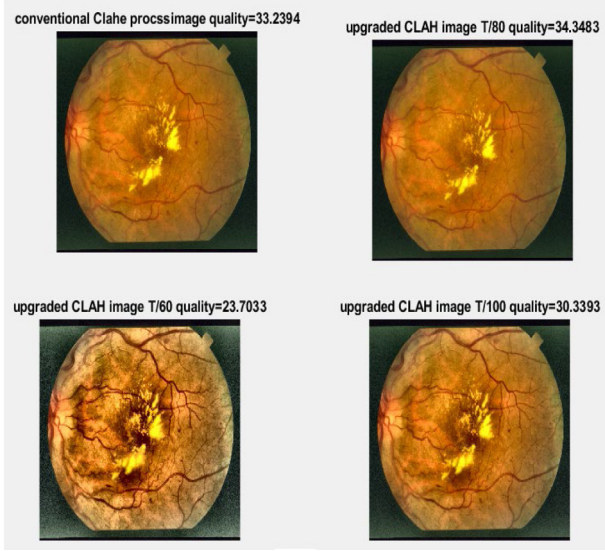


Fig. 4. Fundus image preprocessed by Conventional CLAHE and Upgraded CLAHE with various (T/Th).

2.2.1. CLAHE employed

Several image processing methods had been experimented to process the dataset. However, CLAHE provided the utmost improvement in lifting the prediction accuracy. The CLAHE clipped histogram at a predefined clipping value to avoid excessive contrast enhancement that may result in processed image with odd appearance and undesired artifacts [30]. Moreover, implementation of improper contrast improvement technique could lead to a poor manifestation in vanishing regions, typically the tiny veins. The problem could be overcome with the upgraded CLAHE by adding a global threshold value to the fixed contrast point in the filter. Later, histogram of the targeting image would be improved adaptively according to the pre-defined global threshold value. The outperformance of the improved CLAHE, which overtakes the fixed clipping feature offered by the conventional CLAHE is exemplified in Figs. 4 and 5. Notably, the proposed model greatly improved the image distinctiveness, especially the tiny veins. Subsequently, we conducted normalization to increase wider intensity distribution within a proper range and allow more valuable features to be input into the CNN model. Observing that the images might result in undesirable distortion, see the light ring at the outer border in Fig. 4. The problem could be solved by replacing the region (light ring) with original dark background. The corrective process could be operated in “LAB” color space, and eventually changed the color space back to RGB color space.

Fig. 5 shows the histogram of the resulting images in Fig. 4 that was enhanced with the CLAHE method and the modified CLAHE at T/80. Eq. (1) expressed the clipping limit of the conventional CLAHE, while Eq. (2) explained the controllable threshold value offered by our proposed method.

$$CLIP\ LIMIT = \left\lceil \frac{\varphi}{L} \right\rceil + \left\lceil \beta \cdot \left(\varphi - \left\lceil \frac{\varphi}{L} \right\rceil \right) \right\rceil \quad (1)$$

$$CLIP\ LIMIT = \frac{T}{80} \quad (2)$$

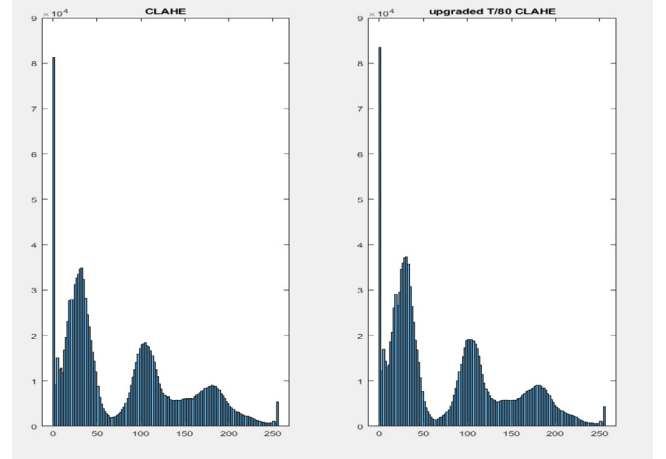


Fig. 5. Histogram of conventional CLAHE-enhanced image (left) and histogram of upgraded CLAHE-enhanced image with a variety T division (right).

where T is the global threshold, φ is the pixels population in each block, β is the clip factor, and L is the gray scale.

2.2.2. Augmentation step

Accuracy of classification of a trained network depends strongly on the training dataset size which consists of adequate of variants. Due to limitation of training data, the augmentation methods are often applied to feed the network. The augmentation applied in this study included the rotation of the dataset images by 30 degrees for eleven times (ranges from 30° to 330°). This stage was taken to feed the CNN network with images of different views and thus forming a trained network that enabled recognition of the region of interest from different orientations. Table 3 shows the numbers of fundus images in the training and validation groups after applying augmentation step.

2.3. Single CNN model

In past decades, different CNN models have been proposed. They are differently designed in terms of the number of convolution layers with different window size, type of kernel filter used, max-pool layer (average and max), solver ('sgdm', 'rmsprop', and 'adam') in training the network, batch sizes, and epochs sizes. The CNN model presented in this paper consisted of convolution layers with depth of 4; while the kernel size used was 3×3 with stride equal to one. In order to preserve the scope of the feature diagrams, one pixel-padding was added. Similar case to the max-pooling layer of size 2×2 where the stride equal to two. At the final stage, the images were compacted to one-dimensional matrix in the fully-connect dense-layers.

The last dense-layer applied the soft-max activation to convert the result into a 1×6 vector in the base model (normal and abnormal), and eventually became 1×2 vector in the classification of images according to their disease classes. The soft-max function converted the output of the fully-connected layer into probability distributions. The classification decisions were made referring to their probability in each disease class.

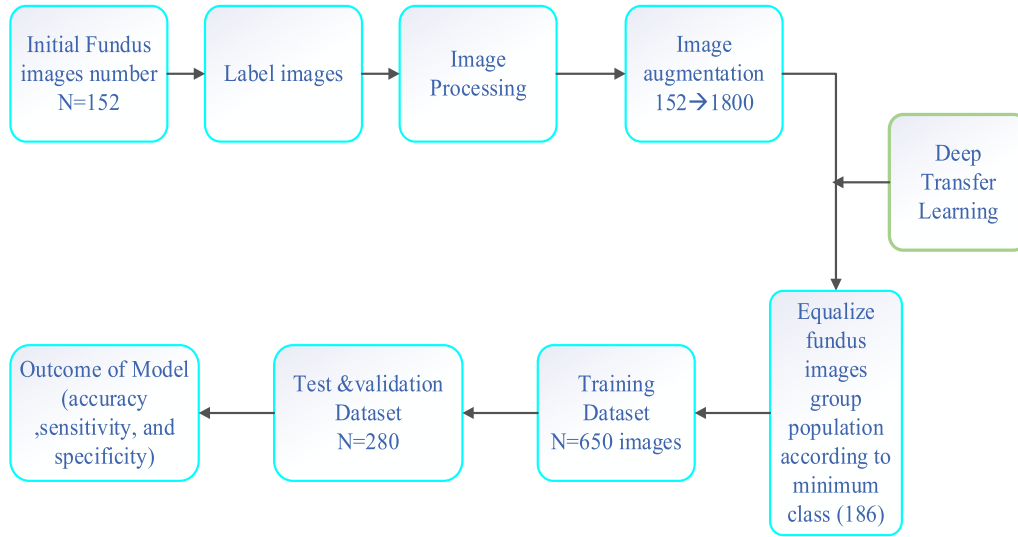


Fig. 6. Flowchart of the proposed approach for categorizing retinal fundus images using the pre-trained network.

In most cases, the main drawback of multi-class classification model is overfitting [31]. Generally, the proposed single CNN network aimed to examine the quality of the enhanced fundus images before entering the following classification stage. A small CNN network was applied at this stage as regular CNN with numerous layers could consume longer time.

2.4. CNN-transfer-learning approach

One of the main contributions added into CNN networks was the combination of the data-store necessities into a single data-store [32]. Inputs of variations were blocked in the single input layer. In most cases, the most widely used pre-trained networks are “Google-Net”, “Vgg16” and “RESNET50”. The major contributors in the pre-trained networks are classifier, feature extractor, and deep-transfer learning. The RESNET50 was proven to have better feature extractions that allowed higher accurate prediction rate as compared to the other CNN networks, which recorded an accuracy score of 67%.

Residual Network “50” was claimed to have more important outcomes than the “Image-Net”. RESNET50 consists of several dimensions of convolutional filters which could minimize the training period and to avoid the over-fitting issue. Therefore, RESNET50 was implemented in this study, given that the network was previously trained with the “Image-Net” database [33]. The images input into the RESNET50 network had size of $224 \times 224 \times 3$, which exemplified width, height, and channel. Later, we applied the transfer-learning for fused feature extraction with the features from the untrained dataset. As a result, the proposed technique potentially assisted the architecture in learning the common features from the raw images without additional training for common data, which indeed minimized the required training time. The merged features were inputted into the new-FC layer for the classifications of background diabetic retinopathy, central retina vein occlusion, choroidal neovascularization, proliferative diabetic retinopathy, and normal case. Fig. 7 showed the proposed fully

connected layer that was specified to have five classes identification and the pre-mentioned pre-trained RESNET50 network on the “Image-Net” data. In fact, full-connected layer [34] consumed the second longest processing than other layers. However, the problem was overcome with the transfer learning concept instead of trained a CNN model from scratch. Fig. 6 showed the overall framework of the proposed automated retinal disease detection model.

3. Results

In deep learning, there are several critical factors to be considered, for example, epochs and learning rate. The best combination of parameters was identified experientially to allow better training performance and classification accuracy. The number of training images used were 650 images, and 280 images for validation from five disease categories. The pictures were arbitrarily separated into training (70%) and test sets (30%). Table 1 showed the accuracy, sensitivity, and specificity of the outputs resulted from the proposed single CNN model that aimed to classify pairs of various retina diseases (BDR: Background Diabetic retinopathy, CRVO: Central retina vein occlusion, CNV: choroidal neovascularization, HIST: Histoplasmosis, PDR: Proliferative diabetic retinopathy and Normal) that had been improved with the proposed upgraded CLAHE.

In the framework of classification presentation, a true positive value (TP) is a result that fittingly forecasts the positive class. Also, a true negative value (TN) is a result that fittingly forecasts the negative class. Meanwhile, false negative value (FN) and false positive (FP) represents the misclassified samples. Implementing these parameters, the equations of the accuracy, specificity and sensitivity can be expressed as follows [35]:

$$Sen = \frac{T_P}{(T_P + T_N)} \quad (3)$$

$$Spe = \frac{T_N}{(T_N + F_P)} \quad (4)$$

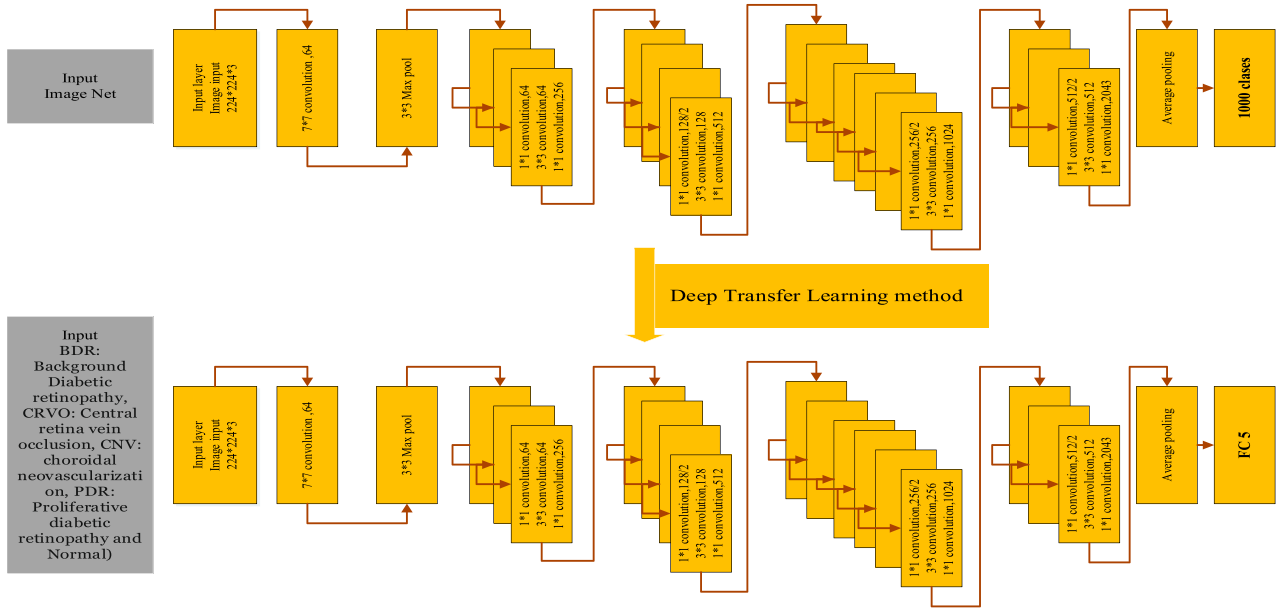


Fig. 7. A sketch to explain the idea of transfer learning concept. (BDR: Background diabetic retinopathy, CRVO: Central retina vein occlusion, CNV: Choroidal neovascularization, PDR: Proliferative diabetic retinopathy and normal case).

Table 1

Output parameters for several single CNN models.

Single CNN	Classified diseases		Accuracy %	Sensitivity%	Specificity%
	A	B			
BC1	CNV_hist	BDR	100	100	100
BC2	PDR	BRV	100	100	100
BC3	CRVO	Normal	100	100	100
BC4	CNV_hist	Normal	100	100	100
BC5	BDR	PDR	100	100	100

$$ACC = \frac{(T_N + T_P)}{(T_N + F_P + T_P + F_N)} \quad (5)$$

From the result obtain through confusion matrix, the proposed model resulted in zero misclassified images, recorded the sensitivity of 100.0% and specificity of 100.0%. As result, the classification model yielded an accuracy rate of 100 percent. Fig. 8 showed clearly that the validation accuracy rose to 100 percent when the parameters were set as follows: 100 epochs, the learning rate at 0.0003, and elapsed time within 262 min, see Table 2. The total images after augmentation became 1800. As the RESNET50 commonly deals with the groups that have identical enumerate images, thus we adjusted the groups' images with a software according to the smallest enumerate image classes of fundus images, which was 186 images and 960 images for training and validation in our case. The classification accuracy of the proposed RESNET50 was shown in Fig. 8. Table 2 displayed the training plot together with the parameters for the transfer-learning RESNET50.

4. Discussion

4.1. Single CNN networks

Deep learning has been magnificently applied in medical image investigation, analyzation, and reconstruction [36].

Nonetheless, disease recognitions in fundus images remain challenging in the recent approaches that involved convolutional neural network (CNN). The proposed single CNN was used as a meter to evaluate the upgraded CLAHE-enhanced images. Referring back to Fig. 4 which displayed four enhanced fundus images with the proposed clipping parameter, the clipping parameter at T/80 was found to achieve the best image enhancement effect according to the validation accuracy test.

Generally, the proposed single CNN framework outperformed in terms of its precision and its great classification accuracy, as shown in Table 1.

4.2. Transfer learning approach

The proposed technique was trained on a modified CNN named RESNET50 [34]. The experimental results outputted from the RESNET50 network were compared and analyzed with set of fused features accompanied by different existing approaches, including feature extraction and transfer learning. The transfer learning method was proven to have the best performance, referring to Fig. 7. The transferred CNN managed to accurately classify the retinal diseases into their respective classes, while the transfer learning method took

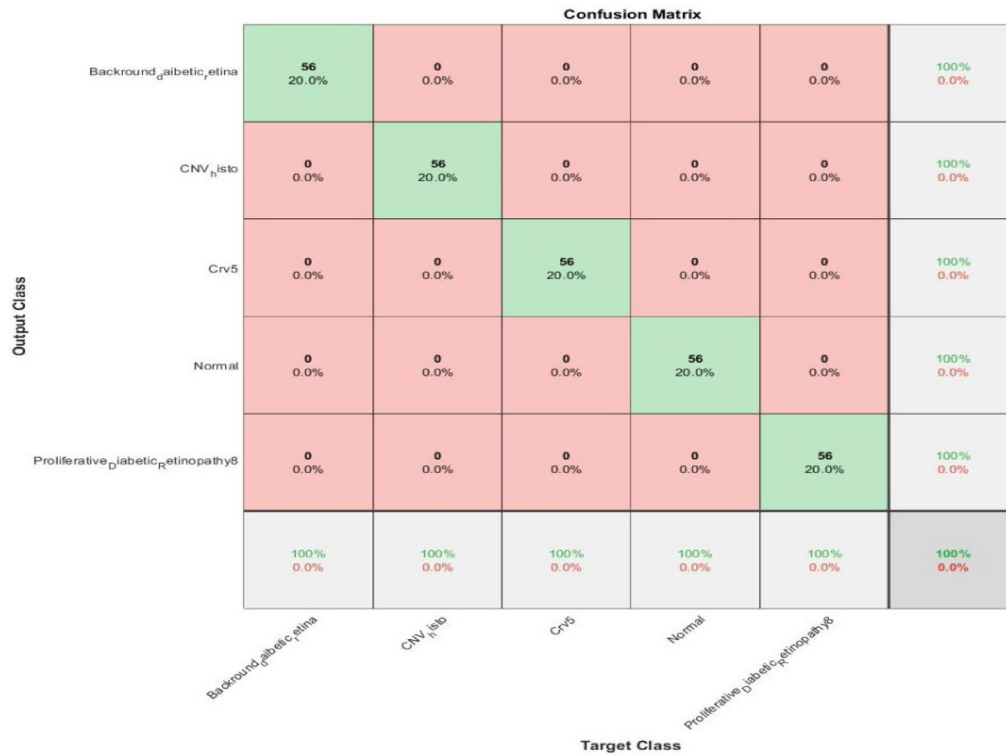


Fig. 8. Confusion matrix for proposed Transferred RESNET50 model.

Table 2

Training Plot values for proposed Transferred RESNET50.

Validation accuracy	Training time	Training cycle (epoch)	Validation frequency	Learning rate
100%	262 min	100	65 iteration	0.0003

Table 3

Distribution of fundus images in the training and validation groups after applying augmentation.

Dataset numbers	Retina illnesses sorts				
	BDR	CRVO	CNV	PDR	Normal
Training	186	186	186	186	186
Validation	56	56	56	56	56

shorter training process instead of training the model from scratch with one thousand classes, as presented in Fig. 8.

Based on Table 2 and Fig. 8, the proposed pre-trained RESNET50 network provides good classification accuracy after augmentation implementation, despite the limitation of available training dataset. The proposed design was competitive with state-of-arts methods introduced in previous studies. The automated detection model using (VGG19) network and (STARE) database proposed in previous study had achieved 95.63% in classification accuracy, 92.99% in validation accuracy and sensitivity ranged from 40 to 100% [31]. Table 4 summarized the strength between the presented work and the previous study. The proposed framework showed superiority

Table 4

Comparison between the proposed model and related work in [31].

Methods	Proposed method	A method in [31]
Number of augmented images	960	2484
CNN	RESNET50	VGG19
Pre-trained Classification accuracy	100%	95.6
Sensitivity	100%	40%–100%
Specificity	100%	99%–100%
Training-set	70%	80%
validation-set	30%	20%
Deep learning technique	Transfer learning	Transfer learning
Epochs	100	50

in terms of its classification accuracy even though the input training dataset was smaller.

Besides the Deep Transferred method, Table 5 shows that proposed model was able to achieve a higher classification accuracy based on deep feature extraction method compared with a previous study in [18].

5. Conclusions

Late treatment or untreated infection leads to blindness. Hence, an early detection of retina infections is crucial. In this paper, upgraded CLAHE technique in improving image

Table 5

Performance of different models tested on STARE dataset using the Feature extraction technique.

Network	Accuracy
Resnet_101 [18]	81.6%
DesNet_121 [18]	85.5%
SetNet_101 [18]	83.21%
WP_CNN_101 [18]	90.84%
Proposed model	96.7%

brightness has been introduced. The enhanced-fundus images were analyzed to diagnose retina illnesses using transfer learning method on CNN (RESNET50) model. The performance of the presented methodology in retinal disease detection revealed superior accuracy as compared to other popular methods. The proposed model was completely independent of the abrupt feature changes thus it could be applied by ophthalmologists in retina illness prediction. However, the proposed model had a drawback that its classification only covered five retina classes. Therefore, further investigation is required to evaluate the model in detecting more disease cases. The superior performance offered by the proposed model could possibly be added into the screening medical devices in viewing retina, such as electrocardiograph, ultrasonic imaging system or other medical detection devices.

Declaration of competing interest

The authors declare that they have no known competing financial interests or personal relationships that could have appeared to influence the work reported in this paper.

Acknowledgment

The study was supported by Universiti Teknologi Malaysia and Fundamental Research Grant Scheme (FRGS), Malaysia, under the grant code R.J130000.7851.5F282.

References

- [1] J. Iveson-Iveson, Anatomy and physiology of the eye, Xianggang Hu Li Za Zhi (35) (1983) 47–50, http://dx.doi.org/10.5005/jp/books/12751_3.
- [2] M. Akil, Y. Elloumi, R. Kachouri, Detection of Retinal Abnormalities in Fundus Image using CNN Deep Learning Networks to Cite this Version: HAL Id : Hal-02428351, 2020.
- [3] Y. Hagiwara, et al., Computer-aided diagnosis of glaucoma using fundus images: A review, Comput. Methods Programs Biomed. 165 (2018) 1–12, <http://dx.doi.org/10.1016/j.cmpb.2018.07.012>.
- [4] X. Zeng, H. Chen, Y. Luo, W. Ye, Automated diabetic retinopathy detection based on binocular siamese-like convolutional neural network, IEEE Access 7 (2019) 30744–30753, <http://dx.doi.org/10.1109/ACCESS.2019.2903171>.
- [5] P. Kaur, S. Chatterjee, D. Singh, Neural network technique for diabetic retinopathy detection, Int. J. Eng. Adv. Technol. 8 (6) (2019) 440–445, <http://dx.doi.org/10.35940/ijeat.E7835.088619>.
- [6] E.A.A. Maksoud, S. Barakat, M. Elmoogy, Medical Images Analysis Based on Multilabel Classification, Elsevier Inc., 2019.
- [7] G.T. Zago, R.V. Andreão, B. Dorizzi, E.O. Teatini Salles, Diabetic retinopathy detection using red lesion localization and convolutional neural networks, Comput. Biol. Med. 116 (2019) 2020, <http://dx.doi.org/10.1016/j.compbiomed.2019.103537>.
- [8] V. Srivastava, R.K. Purwar, Classification of eye-fundus images with diabetic retinopathy using shape based features integrated into a convolutional neural network, J. Inf. Optim. Sci. 41 (1) (2020) 217–227, <http://dx.doi.org/10.1080/02522667.2020.1714186>.
- [9] S.K. Somasundaram, P. Alli, A machine learning ensemble classifier for early prediction of diabetic retinopathy, J. Med. Syst. 41 (12) (2017) <http://dx.doi.org/10.1007/s10916-017-0853-x>.
- [10] M. Hashemzadeh, B. Adlpour, Artificial intelligence in medicine retinal blood vessel extraction employing effective image features and combination of supervised and unsupervised machine learning methods, Artif. Intell. Med. 95 (2018) (2019) 1–15, <http://dx.doi.org/10.1016/j.artmed.2019.03.001>.
- [11] M. Lai, et al., A machine learning approach for retinal images analysis as an objective screening method for children with autism spectrum disorder, EclinicalMedicine (2020) 100588, <http://dx.doi.org/10.1016/j.eclim.2020.100588>.
- [12] D.S.W. Ting, et al., Progress in retinal and eye research deep learning in ophthalmology: The technical and clinical considerations, Prog. Retin. Eye Res. 72 (2018) (2019) 100759, <http://dx.doi.org/10.1016/j.preteyres.2019.04.003>.
- [13] R.S. Biyani, B.M. Patre, Algorithms for red lesion detection in diabetic retinopathy: A review, Biomed. Pharmacother. 107 (July) (2018) 681–688, <http://dx.doi.org/10.1016/j.biopha.2018.07.175>.
- [14] R. Bhattacharjee, M. Chakraborty, Exudates, retinal and statistical features detection from diabetic retinopathy and normal fundus images: An automated comparative approach, in: 2012 Natl. Conf. Comput. Commun. Syst. NCCCS 2012 - Proceeding, 2012, pp. 266–271, <http://dx.doi.org/10.1109/NCCCS.2012.6413019>.
- [15] D.S.W. Ting, et al., Deep learning in estimating prevalence and systemic risk factors for diabetic retinopathy : a multi-ethnic study, npj Digit. Med. (January) (2019) 1–8, <http://dx.doi.org/10.1038/s41746-019-0097-x>.
- [16] E.J. Hwang, et al., Development and validation of a deep learning – based automatic detection algorithm for active pulmonary tuberculosis on chest radiographs, 69, 2019, pp. 739–747, <http://dx.doi.org/10.1093/cid/ciy967>.
- [17] X. Chen, Y. Xu, D. Wing, K. Wong, Glaucoma Detection Based on Deep Convolutional Neural Network, 2015, pp. 715–718.
- [18] J. Hong, et al., Age-related macular degeneration detection using deep convolutional neural network, Futur. Gener. Comput. Syst. 87 (2018) 127–136, <http://dx.doi.org/10.1016/j.future.2018.05.001>.
- [19] S. Otalora, F. Rodríguez, J. Arevalo, F.A. González, A Novel Machine Learning Model Based on Exudate Localization To Detect Diabetic Macular Edema, 2016.
- [20] M. Mohammed, E. Mohammed, M. Jarjees, Recognition of multifont english electronic prescribing based on convolution neural network algorithm, Bio-Algorithms Med-Syst. 16 (3) (2020) 1–8, <http://dx.doi.org/10.1515/bams-2020-0021>.
- [21] P. Chudzik, S. Majumdar, F. Calivá, B. Al-Diri, A. Hunter, Microaneurysm detection using fully convolutional neural networks, Comput. Methods Programs Biomed. 158 (2018) 185–192, <http://dx.doi.org/10.1016/j.cmpb.2018.02.016>.
- [22] J. Krause, et al., Grader variability and the importance of reference standards for evaluating machine learning models for diabetic retinopathy, Ophthalmology 125 (8) (2018) 1264–1272, <http://dx.doi.org/10.1016/j.ophtha.2018.01.034>.
- [23] Y. Jiang, H. Zhang, N. Tan, SS symmetry automatic retinal blood vessel segmentation based on fully convolutional neural networks, 2019, <http://dx.doi.org/10.3390/sym11091112>.
- [24] Y. Joyce Sia Sin, et al., Prominent region of interest contrast enhancement for knee MR images: Data from the OAI, J. Kejuruteraan 32 (3) (2020) 145–155.
- [25] S. Long, J. Chen, A. Hu, H. Liu, Z. Chen, D. Zheng, Microaneurysms detection in color fundus images using machine learning based on directional local contrast, Biomed. Eng. Online (2020) 1–23, <http://dx.doi.org/10.1186/s12938-020-00766-3>.
- [26] D. Le, et al., Transfer Learning for Automated OCTA Detection of Diabetic Retinopathy, pp. 1–9.

- [27] X. Li, T. Pang, B. Xiong, W. Liu, P. Liang, T. Wang, Convolutional neural networks based transfer learning for diabetic retinopathy fundus image classification, (978) 2017.
- [28] E. Prokofyeva, M.B. Blaschko, B. Aires, Convolutional Neural Network Transfer for Automated Glaucoma Identification.
- [29] M. Michael Goldbaum, STructured Analysis of the Retina, U.S. National Institutes of Health, 1996-2004. [Online]. Available: <http://cecas.clemson.edu/ahoover/stare/>.
- [30] C. Liu, X. Sui, Y. Liu, X. Kuang, G. Gu, Adaptive contrast enhancement based on histogram modification framework, 0340, 2019, <http://dx.doi.org/10.1080/09500340.2019.1649482>.
- [31] S. Karthikeyan, P. Sanjay Kumar, R.J. Madhusudan, S.K. Sundaramoorthy, P.K. Krishnan Namboori, Detection of multi-class retinal diseases using artificial intelligence: An expeditious learning using deep CNn with minimal data, Biomed. Pharmacol. J. 12 (3) (2019) 1577–1586, <http://dx.doi.org/10.13005/bpj/1788>.
- [32] G. Van Steenkiste, G. van Loon, G. Crevecœur, Transfer learning in ECG classification from human to horse using a novel parallel neural network architecture, Sci. Rep. 10 (1) (2020) 1–12, <http://dx.doi.org/10.1038/s41598-019-57025-2>.
- [33] M.T. Hagos, S. Kant, Transfer learning based detection of diabetic retinopathy from small dataset, 2019, [Online]. Available: <http://arxiv.org/abs/1905.07203>.
- [34] H. Pratt, F. Coenen, S.P. Harding, D.M. Broadbent, Y. Zheng, Feature visualization of classification of diabetic retinopathy using a convolutional neural network, CEUR Workshop Proc. 2429 (2019) 23–29.
- [35] V. Chandore, Automatic detection of diabetic retinopathy using deep convolutional neural network, 3, 2017, pp. 633–641.
- [36] M. Aubreville, et al., Automatic classification of cancerous tissue in laser endomicroscopy images of the oral cavity using deep learning, Sci. Rep. 7 (1) (2017) 1–10, <http://dx.doi.org/10.1038/s41598-017-12320-8>.